Tuning the luminescence and optical properties of graphene oxide and reduced graphene oxide functionnalized with PVA

Meryem Goumri[1] · Jany Wéry Venturini[2] · Anass Bakour[1,2] · Mohammed Khenfouch[1,3,4] · Mimouna Baitoul[1]

Abstract The attractive optoelectronic properties of graphene are universally known. Also, their combination with polymer matrix added an exciting physical investigation. In the present work, nanocomposites based on poly (vinyl alcohol) (PVA) with low graphene oxide (GO) and partially reduced graphene oxide (PRGO) loadings (0.5, 1 and 2 wt%) were successfully prepared by a simple and environmentally friendly process using aqueous solution in both acidic (pH 4) and neutral media (pH 7)and optimized sonication time, in order to tailor the optical/electronic properties of the GO/PRGO nanosheets. FT-IR and Raman scattering spectroscopy reveal a strong interfacial interaction by hydrogen bonding between the two components. Steady-state photoluminescence results showed a pH-dependent fluorescence of these nanocomposites, and a significant luminescence over a wide range of the visible wavelengths was achieved at a concentration of 1 wt% GO and PRGO loading. A quenching of the PL started at 2 wt% suggesting the possibility of tuning the luminescence properties of GO/PRGO-based composites with PVA.

1 Introduction

Among the different types of nanomaterials, graphene has become the most attractive material, because of its excellent electrical, thermal, mechanical, optical properties, and high transparency with high specific surface area [1–4]. Recently, graphene is considered as one of the most promising nanoscale materials in electronics applications. Several methods for the graphene synthesis were reported including the micromechanical cleavage, epitaxial growth, exfoliation of graphene sheets, thermal and chemical reduction of graphite oxide [5]. In addition, the optoelectrical properties of the graphene film are very sensitive to the number of their layers [6]. However, the graphene is a zero-gap semiconductor, due to the continuous sp^2 hybridized structure, and can be used as a passive element in the optoelectronic applications [7, 8]. The opening of a band gap is possible due to the chemical functionalization of the graphene with the oxygen atom. The formation of sp^2 clusters in the sp^3 matrix is expected to produce quantum confinement effects, which result in the opening of the band gap, at the Fermi level [9]. Graphene oxide (GO) is a modified graphene sheet containing oxygen functional groups (epoxy, hydroxyl and carboxyl) on the basal plane or at the edges [10–12]. One of the interesting properties of GO is its ability to exfoliate spontaneously in aqueous media into individual sheets to form a colloidal suspension [10, 12, 13]. Also, GO has a substantial band gap due to the presence of both sp^2 and sp^3 hybridized

✉ Mimouna Baitoul
baitoul@yahoo.fr

1   Group of Polymers and nanomaterials, Laboratory of Solid state Physics, Faculty of Sciences Dhar el Mahraz, University of Sidi Mohammed ben Abdellah, PO Box 1796, 30 000 Atlas Fez, Morocco

2   Institut des Matériaux Jean Rouxel, CNRS, UMR 6502, Université de Nantes, 2 rue de la Houssiniére, PO Box 3229, 44322 Nantes cedex, France

3   Engineering and Technology Science Campus, UNISA Africa Chair in Nanosciences-Nanotechnology, College of Science, Corner of Christiaan de Wet Road and Pioneer Avenue, Florida, Johannesburg 1709, South Africa

4   iThemba LABS-National Research Foundation of South Africa, Old Faure Road, PO Box 722, Somerset West, Western Cape Province, South Africa

carbon [14–16]. Theoretical studies have shown that in a carbon material containing a mixture of sp^2 and sp^3 carbons, the photoluminescence is determined by the π states of the sp^2 embedded in the sp^3 matrix [17]. The radiative recombination of electron-hole pairs in the sp^2 embedded in the sp^3 matrix can give rise to fluorescence [18–20]. Therefore, the size, shape, and interface surface of sp^2 carbon domains can determine the band gap width and the fluorescence energy [18, 19]. The graphene-based materials give ultraviolet–near-infrared (UV–NIR) fluorescence and exhibit diversity due to the surface functionalization, size of the graphene sheets, and treatment solution [21]. High optical absorption and a broadband fluorescence in the visible–near-infrared (Vis–NIR) spectral regions between (600–1100 nm) wavelengths for GO were reported [20]. Chien et al. have suggested that the predominant emission in GO is from optical transitions between the disorders induced localized states which may be located in the band tail of the $\pi - \pi^*$ or lie deeper within gap leading to a broadband emission [22]. Some researchers tend to exclude the oxygen functional groups as the origin of observed luminescence, because the luminescence was reported to be enhanced with reduction. This inference seems to be questionable, since at the initial stage of GO reduction with hydrazine, some edge groups such as carboxyl groups still remain intact in the structure [23]. However, Gokus et al. [24] have recently observed visible luminescence from oxygen plasma-treated graphene. The GO reduction usually leads to the disappearance of oxygen functional groups and the creation of newly formed small sp^2. Consequently, the electron-hole recombination of these sp^2 cluster-like states exhibited blue fluorescence at shorter wave lengths with a narrower bandwidth [25–27]. It has been reported that aqueous dispersions of GO showed strongly pH-dependent fluorescence [14, 16]. We have reported in our previous work that the GO combined with porphyrin nanorods or Zinc oxide nanorods may generate a white light emission with a near UV excitation [28, 29]. Kundu et al. have reported the photoluminescence from GO-based composites with poly (vinyl alcohol)(PVA) [30].The PVA is known as non-toxic, biodegradable, biocompatible and hydrophilic polymer by hydroxyl groups (–OH), which can interact with the hydroxyl, epoxy and carboxyl groups in the GO. In this work, we report a simple approach, compared to previous works [30], to synthesize nanocomposite films based on PVA and appropriate low contents of GO and partially reduced GO (PRGO) using distilled water and conduct a comparative study on their optical and photoluminescence properties. The aim of this work is to prepare a fluorescent composite material over a wide range of the visible emission and investigate the influence of the GO reduction on the optical properties of the PVA-based

composites at low load (0.5, 1 and 2 wt%). The pH effect on the luminescence properties of these nanocomposites is also reported. Moreover, Raman scattering analysis of these type of nanocomposites was not well enough studied in previous studies; we have used this technique in our present study to gain more detailed understanding of the interaction at the interface of these components and probe the structural change and defects occurring during chemical processing from GO to PRGO and their interaction with PVA.

2 Experimental

2.1 Materials

Graphite was purchased from Sigma Aldrich. Graphene oxide (GO) was obtained by graphite oxidation using modified Hummer's method [10]. Reduction of GO was performed by chemical method using hydrazine hydrate (N_2H_4) as reducing agent. Poly (vinyl alcohol) (PVA) matrix with a molecular weight of 95,000 g/mol used in this study was purchased from Arkema.

2.2 Samples Preparation

2.2.1 Preparation of graphene oxide and partially reduced graphene oxide solutions

A colloidal aqueous suspension of the GO and exfoliated partially reduced GO (PRGO) nanosheets were prepared as follows: Amounts of graphite oxide powder of 5, 10 and 20 mg were dispersed in 3 ml distilled water. Further, ultrasonication method was used for 1 h at a room temperature to obtain GO nanosheets. To prepare PRGO, a solution of hydrazine hydrate (10 %) of the GO dispersion was added with continuous stirring for 48 h at 40 °C. Finally, ultrasonication for 1 h at 40 °C was used to obtain solutions of well exfoliated graphene sheets before their use in the preparation of nanocomposites based on PVA. More details about the high quality and morphology of our GO and RGO prepared by this chemical method using hydrazine [31] have been reported in our previous work [13].

2.2.2 Preparation of GO/PVA and PRGO/PVA nanocomposites

The technique of solution mixing was employed using distilled water for making nanocomposite films based on PVA and two different types of nanofillers such as GO and PRGO nanosheets. Three series of nanocomposite films were prepared separately with GO and PRGO contents of

0.5, 1 and 2 wt%. GO/PVA and PRGO/PVA nanocomposites containing different amounts of the GO and PRGO were prepared as follows: PVA (4 g) was dissolved in 28 ml of deionized water using a magnetic stirrer for 5 h at 80 °C and to prevent the evaporation, sealed containers were used. Then, 7 ml of the PVA solution was added into the GO/PRGO solutions and kept for one hour at a room temperature under uniform stirring. The solution was further agitated on the magnetic stirrer for 48 h under weak stirring to obtain well-dispersed solutions preserving the integrity of the polymeric chains [32]. The obtained homogeneous solutions were slowly drop-casted onto glass substrate and dried at 40 °C . Pure PVA film was also drop-casted from aqueous solution in the same conditions and used as a reference. The solutions in acid medium were prepared using a dilute solution of hydrochloric acid (HCl).

2.2.3 Characterization

Fourier transform infrared spectra were recorded at room temperature in the transmittance mode using a Vertex 70 spectrophotometer, with a resolution of $4\,\mathrm{cm}^{-1}$ over a wave number range of $400-4000\,\mathrm{cm}^{-1}$. Raman spectra were recorded using Raman scattering spectrometer Senterra of Bruker. Spectra were collected between $90-3200\,\mathrm{cm}^{-1}$ with an excitation wavelength of 785 nm, a power of 100 mW and an automatic correction of fluorescence. Optical absorption measurements were recorded using a Varian Cary 5 UV–visible-near-infrared spectrophotometer working in absorption mode in the wavelength range varying from 2000 nm (0.62 eV) to 200 nm (6.2 eV). Steady-state photoluminescence measurements (PL) were performed at room temperature with a "Jobin-Yvon Horiba iHR 320" spectrometer at 420 nm with a filter of 455 nm using a xenon lamp (500 W), and spectra were obtained using a CCD detector.

3 Results and discussion

3.1 Fourier transform infrared spectroscopy (FT-IR)

The functionalization and interaction of GO/PRGO with PVA were followed by FT-IR analysis as shown in Fig. 1a, b. From GO spectrum, graphene characteristic bands and oxygenated functional groups are observed. The band at $1617\,\mathrm{cm}^{-1}$ can be attributed to the elongation of the carbon–carbon bond, and the bands at 2927 and $1417\,\mathrm{cm}^{-1}$ are attributed to the stretching vibration and deformation of the aliphatic C–H groups, respectively. The bands at 1719 and $1041\,\mathrm{cm}^{-1}$ can be attributed to the stretching vibration of C=O and C–O groups, respectively, and the band at $1229\,\mathrm{cm}^{-1}$ can be attributed to the bending vibration of C–OH groups. Moreover, the band at $955\,\mathrm{cm}^{-1}$ can be assigned to the bending vibration of the O–H–O groups. The band at $3213\,\mathrm{cm}^{-1}$ corresponds to the stretching vibration of the hydroxyl group [33]. From PRGO spectrum, the intensity of the bands corresponding to hydroxyl, aliphatic, C=O and C–OH groups decreases indicating the partially reduction of GO [34]. Moreover, the presence of the peaks located at 972, 1017 and $1395\,\mathrm{cm}^{-1}$ corresponding to the bending vibrations of the O–H–O, C–O and C–H groups, respectively, suggests the existence of water trapped between graphene sheets and oxygenated groups located at the edges of the graphene sheets, and the use of hydrazine hydrate also favors the existence of C–H groups. In the pristine PVA spectrum, the stretching vibration of O–H groups was observed at $3288\,\mathrm{cm}^{-1}$. The symmetric and antisymmetric vibrations of $C-H_2$ groups appeared at 2932 and $2916\,\mathrm{cm}^{-1}$ respectively. The peaks at 1417 and $1328\,\mathrm{cm}^{-1}$ were attributed to the deformation vibration of C–H groups, and a peak at $1089\,\mathrm{cm}^{-1}$ corresponds to the stretching vibration of C–O groups. The peak located at $917\,\mathrm{cm}^{-1}$ can be attributed to the stretching vibration of O–H groups [35]. As the GO/PRGO loading increases, the peaks broadening and the ν_{O-H} wavenumber downshift can be attributed to the dissociation of the hydrogen bonds among the hydroxyl groups in PVA molecules, probably due to the interaction with GO and PRGO nanosheets through a hydrogen bond [34].

3.2 Raman spectroscopy

It is recognized that Raman spectroscopy is a powerful technique to characterize reduction and exfoliation of graphene layers. As shown in Fig. 2a, Raman spectrum of GO displays two main bands; the first G band at $1600\,\mathrm{cm}^{-1}$ arises from the stretching of the C–C bond in graphitic materials and is due to E_2g mode at the Γ- point. D band observed at $1332\,\mathrm{cm}^{-1}$ is attributed to structural defects and disorder in graphene nanolayers, and the 2D band is a second-order two phonon process. It appears at double frequency of the D band at $2656\,\mathrm{cm}^{-1}$ [36]. The ratio of D to G bands intensity I_D/I_G was of 0.92. For the PVA, the bands at 2910 and $1435\,\mathrm{cm}^{-1}$ are attributed to stretching and deformation vibrations of C–H groups, respectively. The peak at $1137\,\mathrm{cm}^{-1}$ is ascribed to O–H group vibrations [37].

As shown in Table 1, the intensities ratios (I_D/I_G) for the nanocomposites based on GO and PRGO decrease. This behavior confirms the reduction of defects in GO and PRGO layers and their orientation after the interaction with the PVA
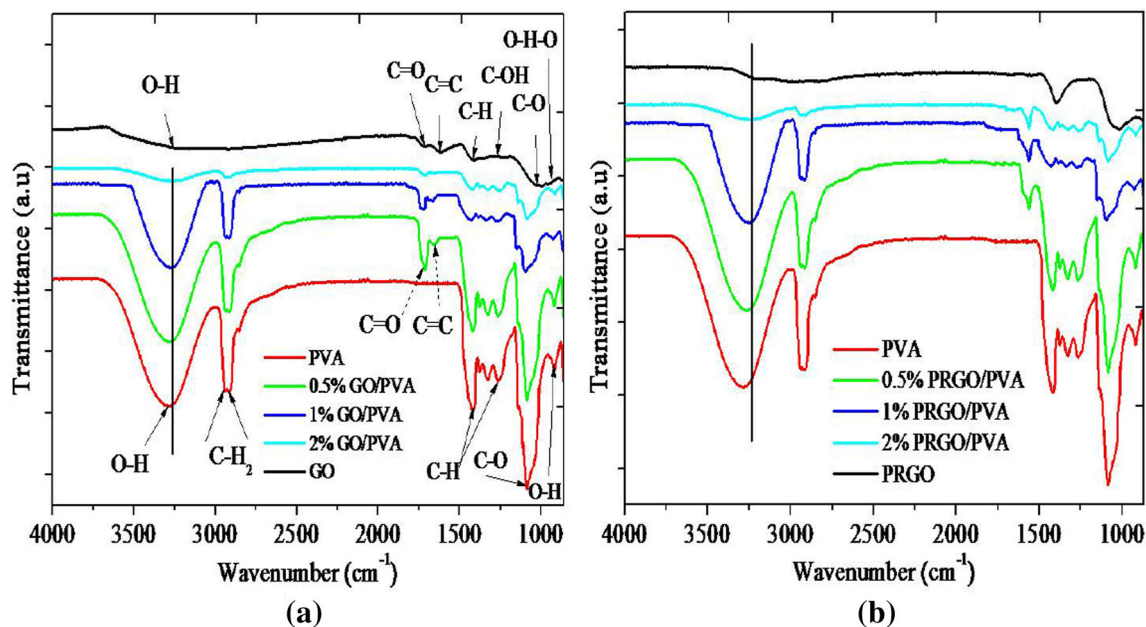
Fig. 1 FT-IR spectra of **a** GO/PVA, **b** PRGO/PVA recorded on the composite films with different concentrations of GO/PRGO
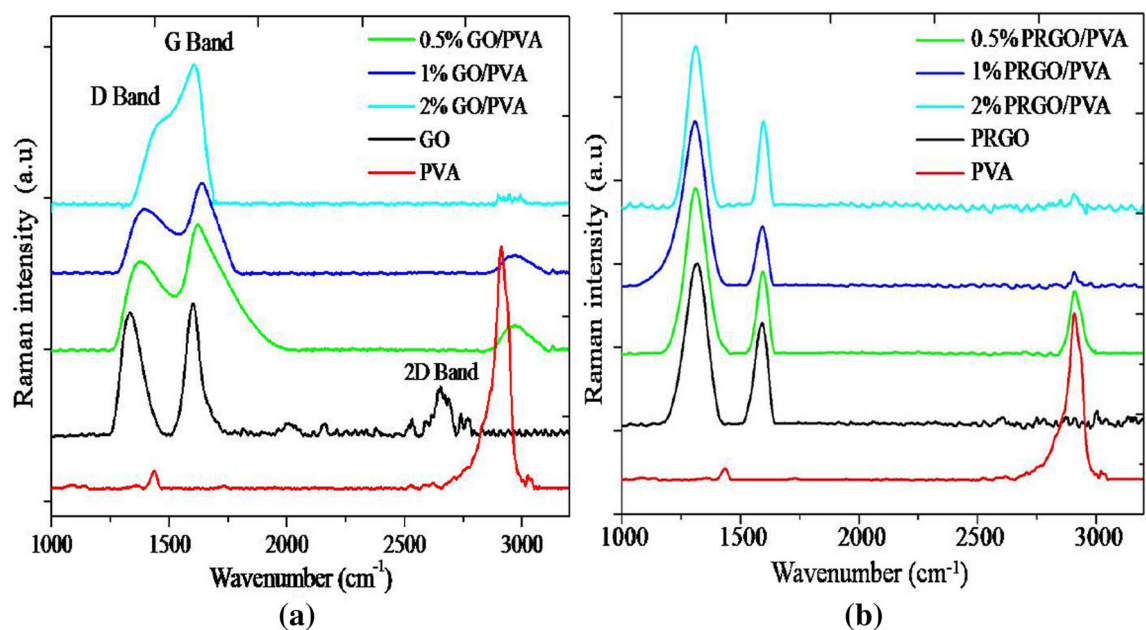

Fig. 2 Raman spectra of **a** GO/PVA, **b** PRGO/PVA nanocomposites with different concentrations of GO/PRGO recorded with 785-nm excitation wavelength

hydroxyl group. The I_D/I_G ratio has been used to qualitatively characterize the change in defects in the carbon nanostructure, which should decrease during the reduction process [25]. In our present work, the intensity ratio of PRGO nanocomposites is higher than that of GO nanocomposites. It can be ascribed to the reduced state which increases the number of aromatic domains of small size in graphene, leading to an increase in the I_D/I_G ratio [36].

The GO/PVA nanocomposites spectra show an upshift of the D and G bands, and the 2D band has completely disappeared. The upshift in the G band frequency can be due to an increase in the elastic constant of the GO/PVA harmonic oscillator. It is highly related to the charge transfer between the GO and PVA. The disappearance of the 2D band is attributed to the presence of the carboxyl functional groups on the surface of the GO, which provided

Table 1 (I_D / I_G) ratios of nanocomposites based on GO and PRGO

	I_D/I_G (GO/PVA)	I_D/I_G (PRGO/PVA)
100 wt%	0.92	3.84
0.5 wt%	0.74	3
1 wt%	0.72	2.87
2 wt%	0.59	1.66

a better adhesion between the hydroxyl groups of PVA matrix and the oxygenated functionalities of the GO [38]. The shape change of D and G bands in GO/PVA nanocomposites spectra is due to the appearance of a new vibration mode located around $1450\,cm^{-1}$, which proves clearly the strong interaction by hydrogen bonding between GO and PVA matrix. In the PRGO/PVA nanocomposites spectra, no shift of the D and G bands was observed which proves no charge transfer between the PRGO and PVA. It can be attributed to the weak interaction by hydrogen bonding between the two components as compared with the GO/PVA. The intensity of the PVA peak in the nanocomposites decreases by increasing the nanofillers concentration. Moreover; the absence of this peak for 2 wt% of GO/PRGO can be attributed to the dissociation of the hydrogen bonds among the hydroxyl groups in PVA molecules after incorporation of the nanofillers.

3.3 Optical absorption

Figure 3 shows the ultraviolet–visible (UV–visible) spectra of PRGO, GO and their nanocomposites with the PVA as matrix. The spectrum of GO has an absorption peak at 237 nm which is upshifted to 270 nm in the PRGO. This redshift is due to the electronic configuration in graphene after the GO reduction. The absorption peaks at 237 and 313 nm can be attributed to $\pi - \pi^*$ and $n - \pi^*$ transition of aromatic C-C ring and C=O bonds, respectively. The absorption peak at 270 nm is attributed to $n - \pi^*$ transition of C-O bonds now embedded by exfoliation and intercalation on the graphene sheets. Also, the disappearance of the shoulder around 313 nm after the GO reduction is most likely due to the removal of carboxyl groups within PRGO [25, 28]. The PVA spectrum has an absorption peak at 189 nm corresponding to the structure of (CH=CH)$_2$–CO– and (CH=CH)–CO–, with a shoulder at 211 nm attributed to (CH=CH)$_4$–CO– structure [39]. The spectrum shows only the ultraviolet absorption bands, as a result, the PVA is transparent.

The absorption peaks are blueshifted with the PVA addition. The peak at 237 nm of the GO has shifted to 220, 215 and 208 nm for 0.5, 1 and 2 wt% GO/PVA, respectively, while the peak at 313 nm has shifted to 280 nm in every cases. Also, the PRGO peak at 270 nm has shifted to 258 and 246 nm for 1 and 2 wt% PRGO/PVA, respectively. The blue shifts may be attributed to the decrease in planarity of the nanosheets due to hydrogen bonds produced between the GO oxygenated functionalities or the residuals functional oxygen groups in the PRGO and the PVA hydroxyl groups [28].

The band gap can be determined at the tangent to the absorption front, and the width of the band gap is strongly
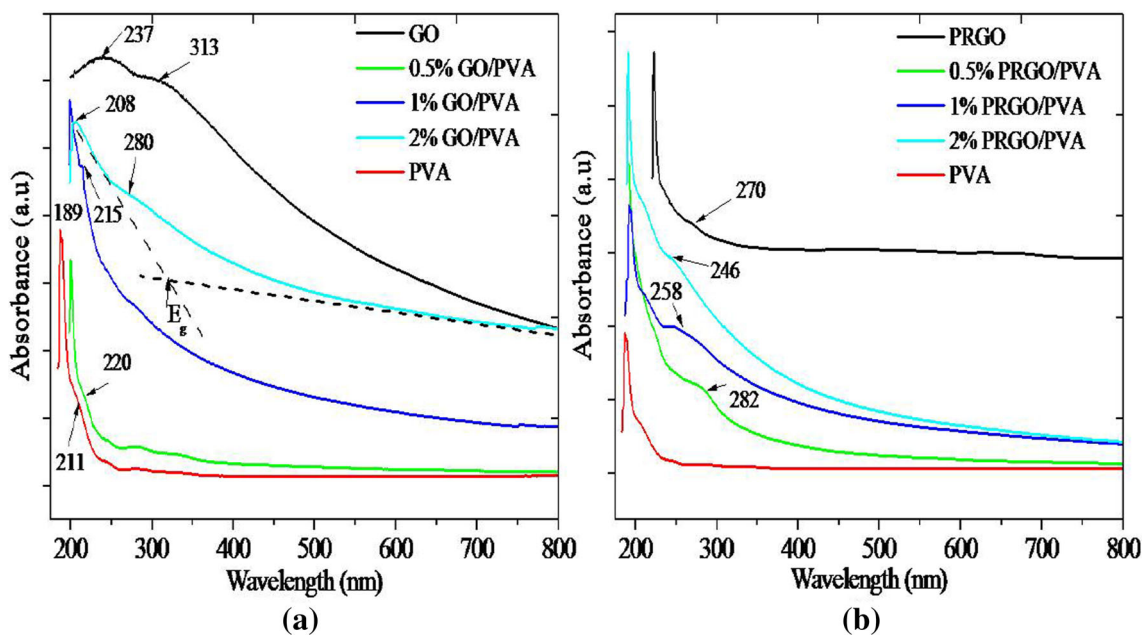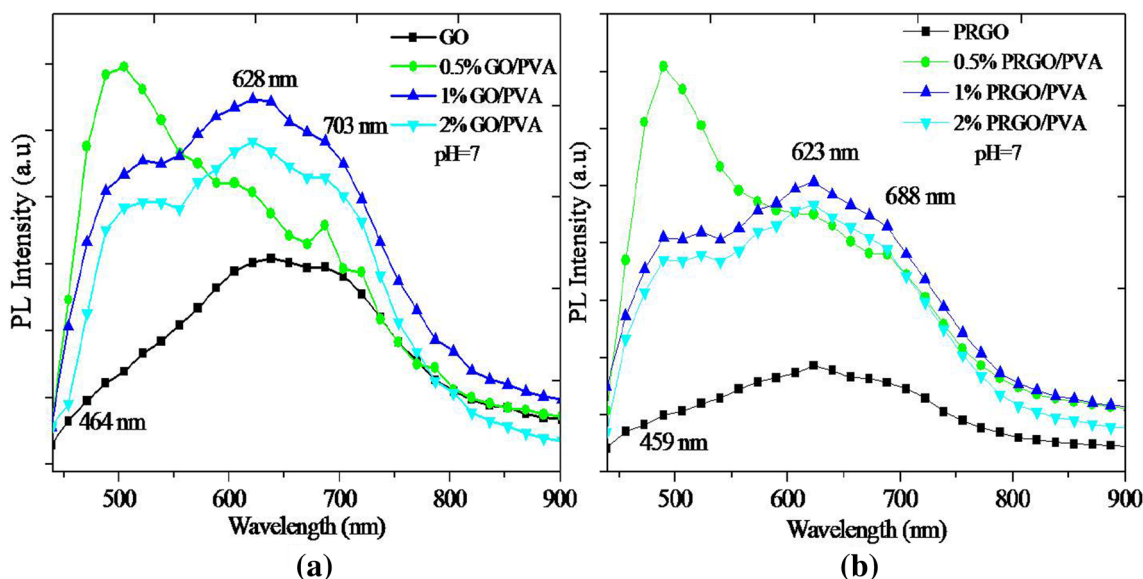

Fig. 3 Optical absorption spectra of **a** GO/PVA, **b** PRGO/PVA composite films

Table 2 Gaps energy of the nanocomposites decrease by increasing of the GO/PRGO concentration

	PVA	GO/PVA			PRGO/PVA		
		0.5 wt%	1 wt%	2 wt%	0.5 wt%	1 wt%	2 wt%
Gap energy (eV)	5.46	5.30	4.36	3.87	5.32	4.42	4.10

Fig. 4 PL spectra of **a** GO/PVA, **b** PRGO/PVA nanocomposites at pH 7 recorded with 420-nm excitation wavelength showing the effect of the PVA addition on composite

dependent on the conjugation length. In fact, when the graphene concentration increases, the extension of the conjugated system and the decrease in the gap energy to lower energies were observed (Table 2).

3.4 Photoluminescence

Figure 4 shows the PL spectra of GO and PRGO with PVA nanocomposite films recorded from 400 to 900 nm for different concentrations at pH 7 with an excitation wavelength of 420 nm. A broad blue–green emission of PVA was observed at 497 nm, and the two peaks at 619 and 683 nm can be attributed to $n - \pi^*$ transitions electrons $2p^2$ (O) in OH groups [40]. The fluorescence from GO was observed at wavelengths of 464, 628 and 703 nm. The photoluminescence of GO is due to electron-hole recombination from conduction band (CB) bottom and nearby localized electronic states to wide-range valance band (VB). In view of atomic structure, the GO emission is predominantly from the electron transitions among/between the non-oxidized carbon region (–C=C–) and the boundary of oxidized carbon atom region (C–O, C=O and O=C–OH) [26, 27]. The weak peak at 464 nm was attributed to the electron-hole radiative recombination in the sp^2 clusters. Thus, the red emission observed around 628 and

703 nm corresponds to oxygen functional groups. However, the sp^2 clusters in GO are lower compared to sp^3 oxygenated regions which can create a very strong fluctuation width of the emission band [25]. However, the partially reduction reduces the emission due to the decreasing of oxygen functionalities. It can be observed that the PRGO luminescence peaks are blueshifted after the partially reduction with (N_2H_4).

The O–H groups dominate after the chemical reduction of GO which favors a blue fluorescence [16]. Also, the GO reduction usually favors sp^2 clusters and leads to the creation of small and newly formed sp^2, which are smaller in size, but numerous and the electron-hole recombination of these sp^2 states exhibited blue fluorescence [22, 25]. The emission bands of the nanocomposites have blueshifted to 459, 623 and 688 nm. The PL intensity of the GO/PRGO-based nanocomposites increases significantly with the PVA addition. This improvement in the fluorescence can be attributed to the functionalization of the GO/PRGO surface, due to the hydrogen bonds produced from various functional groups on the graphene layers with the hydroxyl-rich PVA chains. The decrease in the planarity due to the hydrogen bonding contributes to the decreases in nonradiative recombination of electron-hole, improving thus the emission efficiency of the functionalized graphene [28].
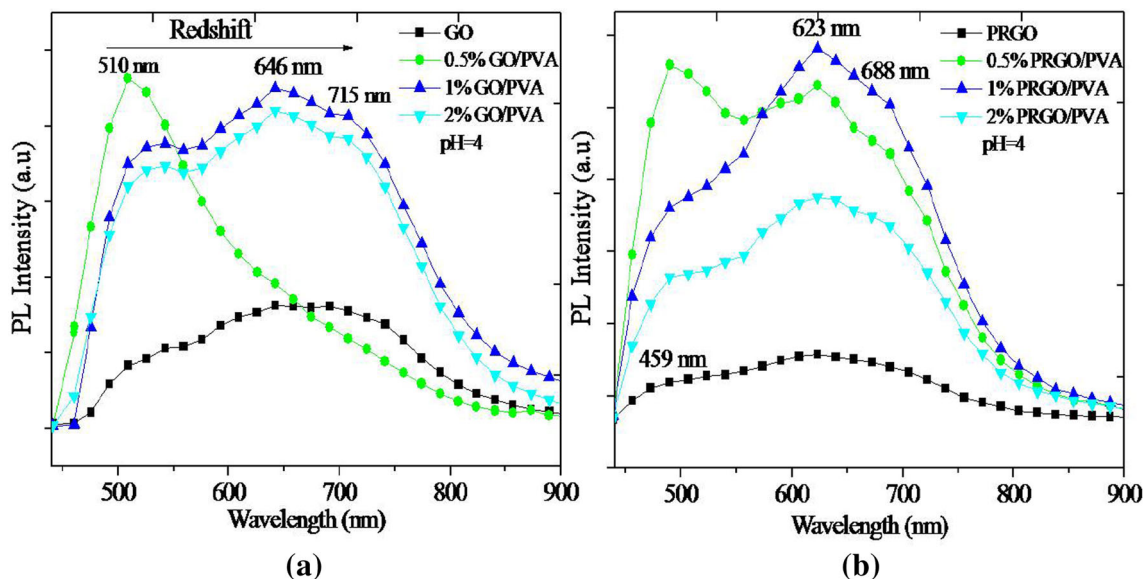
Fig. 5 PL spectra of **a** GO/PVA, **b** PRGO/PVA nanocomposites at pH 4 show a *red* shift originated from pH effect. Excitation: 420 nm

It is observed that an important luminescence over a wide range in blue, green, red emission was observed at concentrations lower than 2 wt% GO/PRGO. As shown in Fig. 5, at pH 4, the GO/PVA spectra display a broad band ranging from 510 nm, 646–715 nm. A monotonic increase and redshift of the emission band were observed for contents of the GO lower than 2 wt%. The origin of the observed fluorescence arises from quasi-molecular fluorophores similar to polycyclic aromatic compounds, formed by the electronic coupling of the COOH groups with nearby carbon atoms of the graphene. Below pH 8, it has been shown that the excited-state protonation of the (G–COO$^-$) to (G–COOH) contributed to the broad redshifted emission under acidic conditions [14, 16].Our results indicate that the fluorescence of PRGO/PVA nanocomposites, shown in Fig. 5b, can be attributed to the removal of some carboxyl groups and formation of O–H polar groups after reduction with hydrazine. Moreover, the PL quenching was achieved for concentration of PRGO lower than for GO/PVA, suggesting more efficient charge/ energy transfers which in agreement with the results obtained by Raman spectroscopy.

4 Conclusion

Nanocomposite based on PRGO (0.5 wt%) dispersed within PVA matrix in acidic media has been found to emit a blue, green to red fluorescence. Similar range of emission was achieved for higher concentration of GO (1 wt%), suggesting that this arises from electronic coupling of carboxylic group with carbon atom of graphene. It can be concluded that the hydrogen bonds between the oxygenated functionalities of the GO/PRGO and the PVA improve the emission efficiency of the resulting nanocomposites for high content of PVA. A strong luminescence over a wide range of the visible emission was detected at 1 wt% GO/PRGO after that a quenching of the PL has been observed at 2 wt%. Moreover, the PL quenching was achieved for concentration of PRGO lower than for GO/PVA composite suggesting more efficient charge/energy transfer which is in agreement with the result obtained by Raman spectroscopy. The strongly pH-dependent fluorescence in the visible range of these nanocomposites was demonstrated. Tuning the luminescence properties of GO/PRGO by functionalization with biocompatible materials opens the way to their integration in many applications and particularly in biosensors and optoelectronic devices.

References

1. K.I. Bolotin, K.J. Sikes, Z. Jiang, M. Klima, G. Fudenberg, J. Hone, P. Kim, H.L. Stormer, Solid State Commun. **146**, 351 (2008)
2. A.A. Balandin, S. Ghosh, W. Bao, I. Calizo, D. Teweldebrhan, F. Miao, C.N. Lau, Nano Lett. **8**(3), 902 (2008)
3. C. Lee, X. Wei, J.W. Kysar, J. Hone, Science **321**, 385 (2008)
4. M.D. Stoller, S. Park, Y. Zhu, J. An, R.S. Ruoff, Nano Lett. **8**(10), 3498 (2008)
5. H. Kim, A.A. Abdala, C.W. Macosko, Macromolecules **43**, 6515 (2010)

6. A.C. Ferrari, J.C. Meyer, V. Scardaci, C. Casiraghi, K.S. Novoselov, S. Roth, M. Lazzeri, A.K. Geim, F. Mauri, S. Piscanec, D. Jiang, Phys. Rev. Lett. **97**(18), 187401 (2006)

7. K.S. Novoselov, Y. Zhang, A.K. Geim, S.V. Dubonos, S.V. Morozov, I.V. Grigorieva, D. Jiang, A.A. Firsov, Science **306**, 666 (2004)

8. F. Bonaccorso, Z. Sun, T. Hasan, A.C. Ferrari, Nat. Photonics **4**, 611 (2010)

9. H.K. Jeong, C. Yang, B. Kim, K.J. Kim, Europhys. Lett. **92**, 37005 (2010)

10. F.T. Thema, M.J. Moloto, E.D. Dikio, N.N. Nyangiwe, L. Kotsedi, M. Maaza, M. Khenfouch, J. Chem. **2013**, 1 (2013)

11. A. Lerf, H. He, M. Forster, J.J. Klinowski, J. Phys. Chem. B **102**, 4477 (1998)

12. S. Stankovich, D.A. Dikin, R.D. Piner, K.A. Kohlhaas, A. Kleinhammes, Y. Jia, Y. Wu, S.T. Nguyen, R.S. Ruoff, Carbon **45**, 1558 (2007)

13. M. Khenfouch, U. Buttner, M. Baitoul, M. Maaza, Graphene **3**, 7 (2014)

14. C. Galande, A.D. Mohite, A.V. Naumov, W. Gao, L. Ci, A. Ajayan, H. Gao, A. Srivastava, R.B. Weisman, P.M. Ajayan, Sci. Rep. **85**, 1 (2011)

15. J. Shang, L. Ma, J. Li, W. Ai, T. Yu, G.G. Gurzadyan, Sci. Rep. **792**, 1 (2012)

16. S.K. Cushing, M. Li, F. Huang, N. Wu, Acs Nano. **8**, 1002 (2014)

17. K.A. Mkhoyan, A.W. Contryman, J. Silcox, D.A. Stewart, G. Eda, C. Mattevi, S. Miller, M. Chhowalla, Nano Lett. **9**, 1058 (2009)

18. N. Tomozeiu, J. Seekamp, A. Ferrari, J. Niemann, J. Optoelectron. Adv. M. **2**, 241 (2000)

19. D.P. Manage, *Degree of Doctor of Philosophy*, Department of Physics, University of Toronto (1998)

20. Z. Luo, P. Vora, E.J. Mele, A.T.C. Johnson Jr., J.M. Kikkawa, App. Phys. Lett. **94**, 1 (2009)

21. H.R. Thomas, C. Vall, R.J. Young, I.A. Kinloch, N.R. Wilson, J.P. Rourke, J. Mater. Chem. C **1**, 338 (2013)

22. C.T. Chien, S.S. Li, W.J. Lai, Y.C. Yeh, H.A. Chen, I.S. Chen, L.C. Chen, K.H. Chen, T. Nemoto, S. Isoda, M. Chen, T. Fujita, G. Eda, H. Yamaguchi, M. Chhowalla, C.W. Chen, Angew. Chem. Int. Edit. **51**, 6662 (2012)

23. G. Eda, Y.Y. Lin, C. Mattevi, H. Yamaguchi, H.A. Chen, I.-S. Chen, C.-W. Chen, M. Chhowalla, Adv. Mater. **22**, 505 (2010)

24. T. Gokus, R.R. Nair, A. Bonetti, M. Bohmler, A. Lombardo, K.S. Novoselov, A.K. Geim, A.C. Ferrari, A. Hartschuh, Acs Nano. **3**, 3963 (2009)

25. T.V. Cuong, V.H. Pham, Q.T. Tran, S.H. Hahn, E.W. Shin, E.J. Kim, J.S. Chung, Mater. Lett. **64**, 399 (2010)

26. J.R. Rani, S.-J. Kim, J. Oh, J. Park, J. Lim, B. Park, K. Kim, S. Chan, Nanoscale **5**, 5620 (2013)

27. L. Tang, R. Ji, X. Li, G. Bai, C.P. Liu, J. Hao, J. Lin, H. Jiang, K.S. Teng, Z. Yang, S.P. Lau, Acs Nano **8**(6), 6312 (2014)

28. M. Khenfouch, J. Wéry, M. Baitoul, M. Maaza, J. Lumin. **145**, 33 (2014)

29. M. Khenfouch, J. Wéry, M. Baitoul, M. Maaza, Opt. Mater. **34**, 1320 (2012)

30. A. Kundu, R.K. Layek, A. Kuila, A.K. Nandi, A.C.S. App, Mater. Interfaces **4**, 5576 (2012)

31. P.G. Ren, D.X. Yan, X. Ji, T. Chen, Z.M. Li, Nanotechnology **22**, 1 (2011)

32. A. Yasmin, J.-J. Luo, I.M. Daniel, Compos. Sci. Technol. **66**, 1179 (2006)

33. S. Morimune, T. Nishino, T. Goto, Polymer J. **44**, 1056 (2012)

34. C. Bao, Y. Guo, L. Song, Y. Hu, J. Mater. Chem. **21**, 13942 (2011)

35. J. Wang, X. Wang, C. Xu, M. Zhang, X. Shang, Polym. Int. **60**, 816 (2011)

36. J. Guo, L. Ren, R. Wang, C. Zhang, Y. Yang, T. Liu, Compos. Part B Eng. **42**, 2130 (2011)

37. I.Y. Prosanov, A. A. Matvienko, Phys. Solid State **10**(52), 2203 (2010)

38. N. Lachman, C. Bartholome, P. Miaudet, M. Maugey, P. Poulin, H.D. Wagner, J. Phys. Chem. C **113**(12), 4751 (2009)

39. D.M. Sabara, J.S. Dunne, A.Q.H. Pedro, J. Trifunovic, I.I.O. Balogun, A. Serrano, I. Kertész, O. Kotlicic, Biotechnol. Food Sci. **75**, 39 (2011)

40. S. Ram, T.K. Mandal, Chem. Phys. **303**, 121 (2004)